

## FINAL REPORT – NF67576

### Objective of the project

The aim of the project was to identify and characterize the plant components which are essential in the later stages of nodule development, rhizobial invasion and symbiosome function. In order to dissect the later stages of the symbiotic nitrogen fixing interaction between *Sinorhizobium meliloti* and *Medicago truncatula*, mutants with ineffective (Fix-) symbiotic phenotypes have been identified in a screen of fast neutron and EMS mutagenized *M. truncatula* plants. The ineffective symbiotic phenotype was identified by development of white non-fixing nodules, symptoms of nitrogen starvation and retarded growth. Ten Fix- mutant lines (5L, 6V, 7Y, 9F, 11S, 12AA, 13U, 14S, EMS6:T4 and EMS15) which form white ineffective nodules have been selected to analyze their mutant phenotype in details and clone the mutated genes.

### Genetic analysis of ineffective mutants

EMS6:T4 and EMS15 mutant lines had low vigor and due to the poor success rate of crosses with these mutants we could not generate F1 hybrid plants with other Fix mutants or A17 (backcrossing) and A20 (mapping population) plants. Therefore eight Fix- mutant lines (5L, 6V, 7Y, 9F, 11S, 12AA, 13U and 14S) were analyzed further on. In order to determine the allelic relationship of the Fix- mutants we performed genetic crosses between the mutant lines to be analyzed in this project and other previously identified Fix- mutants. The analysis of the symbiotic phenotype of F1 hybrid plants of the crosses between the eight mutant plants revealed that mutants 5L and 11S are allelic while the other six mutants represent distinct complementation groups (Table 1). We also tested the allelic relationship between our and the previously identified ineffective *dnf1-7* (*do not fix*) mutants (Starker et al. 2006); the Fix- phenotype of the F1 progeny of the cross between 6V and *dnf7* and between 14S and *dnf5* mutants revealed that they are allelic (Table 1). Mutants 9F and 12AA belong to different complementation groups from all *dnf* mutants while the complementation test between 5L/11S, 7Y and 13U and the *dnf* mutants was incomplete due to the poor success rate of crosses onto certain mutant plants. As Table 1 shows the 5L/11S mutants are not allelic with *dnf1*, 2, 4, 5 and 7 and 7Y is not allelic with *dnf1*, 4 and 7. The allelism test also revealed that 13U and *dnf2* are mutated in different genes (Table 1).

We crossed the mutant lines to wild type Jemalong plants to generate back crossed populations and analyzing the segregation ratio of the symbiotic phenotypes we found that all the eight mutant loci in behaved as a single recessive locus.

Recipient/pollinator	5L	6V	7Y	9F	11S	12AA	13U	14S	<i>dnf1</i>	<i>dnf2</i>	<i>dnf3</i>	<i>dnf4</i>	<i>dnf5</i>	<i>dnf6</i>	<i>dnf7</i>
5L	■	+(6/2)	+(7/2)		-(6/2)					+(11/3)					+(4/1)
6V		■	+(3/1)			+(3/1)		+(6/2)		+(5/2)					-(9/4)
7Y			■	+(4/2)		+(2/1)	+(8/2)								+(15/4)
9F				■	+(7/2)	+(3/1)	+(5/2)		+(8/2)	+(8/3)	+(9/3)	+(10/3)	+(7/2)	+(8/2)	+(7/2)
11S					■	+(4/2)	+(6/2)	+(9/3)	+(7/2)						
12AA						■		+(7/3)	+(2/1)	+(10/3)	+(23/5)	+(4/2)	+(6/2)	+(9/3)	+(12/3)
13U							■	+(4/2)		+(3/2)					
14S								■	+(6/4)	+(5/4)	+(6/1)	+(11/3)	-(20/4)	+(14/3)	+(18/3)
<i>dnf1</i>									■						
<i>dnf2</i>										■					
<i>dnf3</i>											■				
<i>dnf4</i>												■			
<i>dnf5</i>													■		
<i>dnf6</i>														■	
<i>dnf7</i>															■

Table 1. Allelism tests between Fix- mutants of *M. truncatula*. The plus sign indicates that nodules were Fix+ (complementation), minus sign indicates that nodules were Fix- (lack of complementation) on the F1 hybrid plants. The number of plants scored/number of crosses is shown in parenthesis. The identified allelic relationships are indicated with grey shading.

### Genetic mapping of mutant loci

We have generated F2 mapping populations with crossing the mutant lines to the A20 genotype to determine the map position of the Fix- loci. Due to the poor success rate of genetic crosses with the mutant EMS6:T4 we could not establish an F2 segregation population for this mutant. F2 mapping population was established for the EMS15 mutant but the identification of the Fix- symbiotic phenotype among the F2 plants was not clear-cut which hampered the genetic mapping of the EMS15 mutant locus. The genetic mapping of the other Fix- locus identified their rough map position:

5L and 11S - linkage group 6 (LG 6) between genetic markers MtB267 and AW573833

6V – LG 7 between markers h2\_16n21f and h2\_156l8a (6.6 cM genetic distance)

7Y – LG 7 between markers h2\_16n21f and h2\_30n12a (10.5 cM genetic distance)

9F – LG 5 between microsatellite markers MtB93 and MtB108 in a 7.6 cM genetic distance)

12AA – LG 7 between markers MtB326 and DK296L (11.3 cM genetic distance)

13U – LG 4 between markers MtB69 and DENP (5.7 cM genetic distance)

14S - LG 3 between markers PRTS and EST400 (0.7 cM genetic distance)

## **Morphological studies and characterization of ineffective mutants**

Microscopic analysis, acetylene reduction assay and expression analysis of several nodule specific genes were carried out in order to determine what stages the symbiotic process is blocked.

Analysis of the effectiveness of the nitrogenase activity in the ineffective mutants: To differentiate between mutants defective in the development of the symbiotic interaction with those defective in nutrient exchange we undertook acetylene reduction assay that measures the activity of bacterial nitrogenase. Eight mutants (5L, 6V, 7Y, 9F, 11S, 13U, 14S and EMS15) showed complete absence of nitrogenase activity in their nodules, mutant 12AA showed significant reduction in nitrogenase activity. The absence of nitrogenase activity or the low level of effectiveness of symbiotic nitrogen fixation indicated that our mutants had defects in forming the symbiotic interaction rather impaired in metabolic pathways.

Analysis of nodulation phenotype by light microscopy: in order to determine whether rhizobia were released in the mutant nodules cells we inoculated the *M. truncatula* wild type and mutant plants with *S. meliloti* 1021 (pXLGD4) which constitutively expresses the *LacZ* gene. To visualize the presence of bacteria in the nodules we stained thin longitudinal sections of 21-day-old nodules following inoculation (dpi) for  $\beta$ -galactosidase activity. The extent of bacterial colonization in the nodule zones was examined by light microscopy and micrographs of the sections are shown in Figure 1. The X-gal staining showed the typical zonation (meristematic, invasion, inter, nitrogen fixing and senescence zones) of a fully developed indeterminate nitrogen fixing nodule on wild type *Medicago Jemalong* plants (Fig 1A). No characteristic zonation of the indeterminate nodules was observed in nodules of 9F and 14S (Fig 1B and C). Moreover mutant 9F formed two types of nodules: small uninfected primordia-like structures in which the infection thread development was prematurely arrested in the cortical cells and elongated-type nodules filled with a network of infection threads developed. The nodules of other mutants were further developed and had distinct zones of the small meristematic cells with dense cytoplasm in the distal part of the nodules, medium-sized cells in the infection and interzone and large cells in the nitrogen-fixing zones in the central part of the nodules. Bacteria were detected only in few infection threads (Fig 1D) in the infection zone of 7Y nodules and occasionally a number of cells contained bacteria in the nitrogen-fixing zone but the cells in the central part of the nodule remained actually uninoculated. Moreover

an extensive brown pigmentation was observed in the infection and nitrogen-fixing zone of the 7Y nodules. Mutants 5L and 11S developed nodules with narrow infection zone with several inoculated cells and with a central part containing numerous large uninfected cells and some cells showing indistinct patchy X-gal staining and brown pigmentation which indicates the disintegration of the cytoplasm and the induction of early senescence of the nodules (Fig 1E and F). Staining with X-gal detected bacteria mainly in the infection zone and less in the interzone of the 12AA nodules but no infected cells were found in the central part of these nodules (Fig 1G). The 13U nodules showed lacZ activity in the infection zone and a diffused blue staining was detected occasionally in the nitrogen fixation zone (Fig. 1H). The 6V nodules showed similar occupancy of the cells in the invasion zone to wild type nodules but the nitrogen-fixing region was not filled with blue-staining bacteria at all (Fig. 1I).

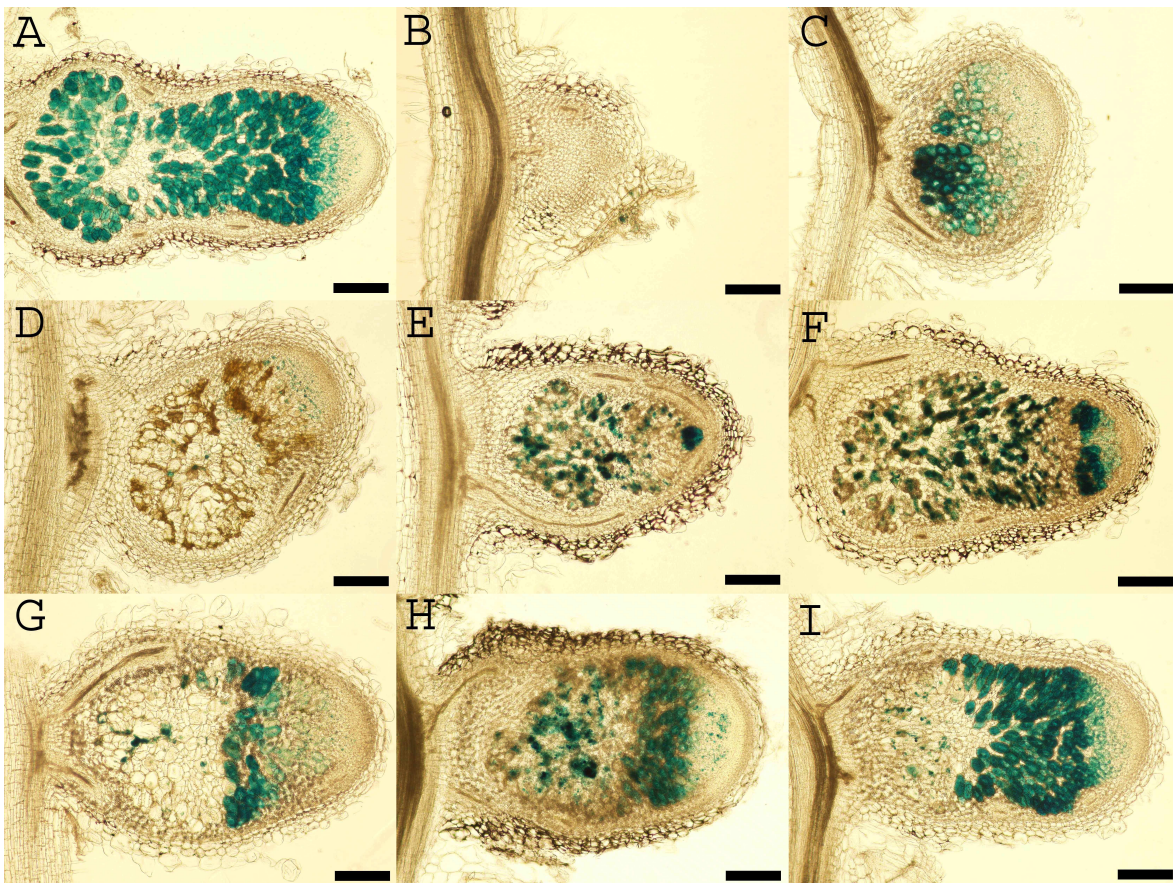


Figure 1. Nodulation phenotypes of ineffective mutant and wild type Jemalong plants. Plants were grown in plates containing Gibson medium and inoculated with *S. meliloti* expressing the *LacZ* gene. 60  $\mu\text{m}$  thick nodule sections were prepared with a vibration microtome and stained for X-gal at 21 days post inoculation (dpi). (A) Wild type Jemalong plant, (B) 9F small nodule, (C) 14S, (D) 7Y, (E) 5L, (F) 11S, (G) 12AA, (H) 13U, (I) 6V. Scale bars represent 200  $\mu\text{m}$ .

In order to examine the brown pigmentation in the 7Y nodules more thoroughly, we analyzed the autofluorescence in the nodules and stained the nodules sections with toluidine blue. For autofluorescence analysis nodules were stained with the nucleic acid binding fluorescent dye, SYTO13 which detects the bacteria in nodules cells. Nodules were viewed with laser scanning confocal microscopy and the rhizobia which bound the fluorescent dye were detected in the green spectrum while cell walls accumulated polyphenolic substances were examined in the red spectrum. No fluorescent phenolic compounds were detected in wild type Jemalong (Fig. 2A) and other mutant plants (Fig. 2C and E) but the invasion and nitrogen-fixing zones in the 7Y nodules appeared in red due to the accumulation of phenolic substances. These data were confirmed with toluidine blue staining. Toluidine blue is a metachromatic dye which stains various tissues different colours depending on their component. Non-lignified primary cell walls are stained purple while cell walls containing phenolic compounds, such as lignin and tannin give green colours. Staining of mutant and wild type nodules with toluidine blue detected strong accumulation of polyphenolics substances in the invasion and the nitrogen fixation zone of 7Y nodules (Fig. 2H) and sporadic green staining in the nitrogen fixing zone of 12AA nodules (Fig. 2B). The detected autofluorescent and toluidine blue stained polyphenolic compounds suggested the strong defence response to rhizobia in the 7Y mutant.

We further investigated the progression of the infection process in nodules of 9F mutant using the fluorescent nucleic acid binding dye SYTO 13. At 18 days post inoculation, images were taken in the nitrogen fixation zone of nodules and plant cells were examined for the presence of rhizobia. Analyzing the images with higher magnification of the extended invasion zone, we detected that bacteria retained in infection threads in 9F nodules and these infection threads displayed abnormal morphology; they were thick and highly crooked with enlarged, blister-like formations (Fig. 2D) compared to wild type infection threads.

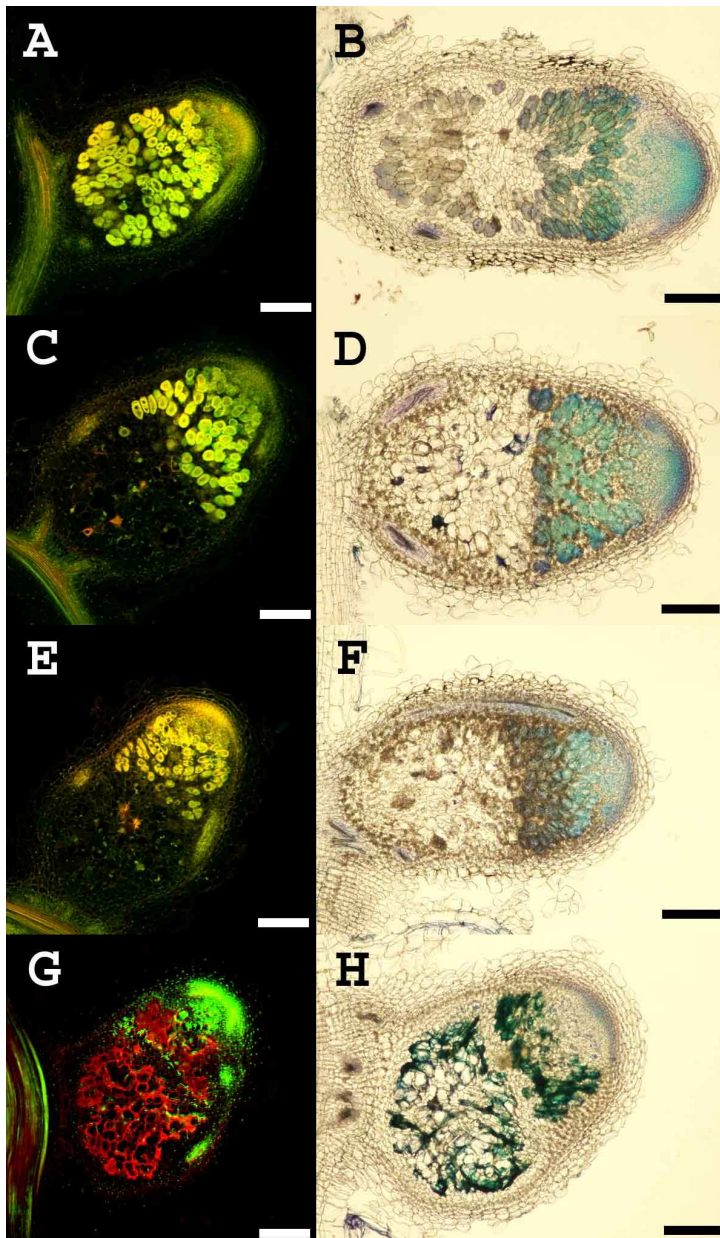


Figure 2. Autofluorescent analysis (A, C, E and G) and toluidine blue staining (B, D, F and H) of wild type Jemalong (A and B) and mutant (C and D-12AA; E and F - 13U; G and H - 7Y) *M. truncatula* nodules 21 dpi with *S. meliloti*. Scale bars represent 200  $\mu\text{m}$ .

Analysis of nodulation phenotype by electron microscopy: ultrathin sections prepared in the nitrogen fixation zone of wild type and mutant nodules were analyzed by transmission electron microscopy (TEM) 18 dpi. Wild-type nodule cells displayed normal ultrastructural organization characteristic for *M. truncatula* cells which were fully packed with bacteroids. 9F nodules contained cells non-invaded by bacteria while 14S nodule cells with small number of non-differentiated rhizobia. In the case of 9F the non-released bacteria were localized in infection threads with irregular thick cell walls and tortuous plasma membrane was often detected surrounding the thickened cell wall of infection threads which was never observed in wild type nodules. The nodules of other mutants contained large number of disintegrated bacteria and plant symbiotic structures which indicated the non-proper accommodation of the symbiotic partner and the early senescence of nodules. The 12AA nodule cells contained numerous cells fully packed

with bacteroids which suggest that this mutant is probably impaired in the normal functioning of the symbiotic interaction.

Transcriptional analyses of *FIX*- mutants: we examined the expression of symbiotically regulated genes in wild type plants and in the *Fix*- mutants. Quantitative RT-PCR experiments were performed on the cDNA samples from roots after 21 days of inoculation with *S. meliloti* 1021. We analyzed the expression profile of nodule specific or nodule enhanced genes (genes encoded an *MtN1*-like protein, *MtN9*, *ENOD2*, *MtN6*, *Mt0344*, *LEC4*, *NOD25*, leghemoglobin (*Lb*) and *NOD26*). Based on the expression profile the symbiotic interaction is blocked in an early phase in mutant 9F and 14S which correspond to the microscopic analyses, while 5L, 6V, 7Y, 11S, 12AA and 13U has defect in a later developmental phase and showed significant reduction of expression of certain nodulin genes indicating specific developmental arrest in the symbiotic process. Mutant 14S showed complete reduction in *NOD26* expression, reduced expression of *MtN1*-like gene, *MtN6*, *Mt0344*, *LEC4*, *NOD25* and *Lb* but showed similar expression of *MtN9* and *ENOD2* as wild type plants.

*The microscopic and transcriptional characterization of the ineffective mutants showed that nodules on 9F and 14S mutants did not show the proper zonation of the indeterminate symbiotic nodules and these mutants were impaired in the invasion of the nodule cells by bacteria. Aberrant infection process was detected in mutant 9F and larger magnification revealed that bacteria were did not release from the infection threads of 9F. The other mutants showed defects in bacteroid differentiation, displayed disintegration of the symbiotic structures or are probably impaired in functioning of the symbiotic nodule (12AA). Mutant 7Y showed high accumulation of polyphenolic compounds indicating strong defense reaction against the rhizobia.*

## Cloning of *FIX* genes

Identification of *FIX* genes were attempted by either classical positional cloning strategy or the combination of a fine mapping project with an Affymetrix gene chip-based cloning approach.

Positional cloning of mutant genes in 9F, 14S and 7Y mutant lines: Initially the mutant locus was positioned on the upper arm of chromosome 5 (LG 5) between microsatellite markers MtB108 and MtB93. The fine mapping determined the map location of the 9F locus into a genomic region covered by BAC clones mth4-3n15 (accession no. CU914135) and mth4-28c15 (CU469555) using more than 450 F2 plants from the cross of the 9F mutant and A20 ecotype. Intron targeted markers were designed based on predicted coding sequences on these two BAC clones and genetic markers generated for the *GTP* (Golgi transport related protein) and the *BRL* (*BREVIS RADIX like*) genes identified a genomic region of 152 kb length for the 9F locus. Oligonucleotide primers were synthesized for the seven predicted genes in the 9F region and PCR reactions were performed to amplify genomic DNA and cDNA samples prepared from the 9F mutant plant. The amplification of a part of the *IPD3* gene detected a deletion in the *IPD3* transcript. The *IPD3* gene had been identified previously in a yeast two hybrid screen interacting with the DMI3 (Messinese et al. 2007), the member of the Nod factor signaling pathway. Sequence analysis of the *IPD3* cDNA revealed that the entire fourth exon of *IPD3* was missing in mutant 9F. The sequence analysis of 9F genomic DNA identified a single base pair change and 6 bp deletion at the junction of the fourth exon and fourth intron in *IPD3* which causes imperfect splicing and a transcript lacking exon 4. The deletion of the fourth exon of the *IPD3* transcript generates a frame-shift and an immature translational termination in the exon 5 and thus the mutant transcript encodes a truncated protein with additional 8 non-*IPD3* specific residues following the third exon. The predicted incomplete gene product is terminated at the end of the predicted  $\alpha$ -helix structures of *IPD3* and lacks for the terminal nuclear localization signal (NLS) segments and region determined to be sufficient for the interaction with DMI3 therefore the 9F mutant probably has a non-functional *IPD3*. We introduced the *IPD3* transcript driven by the native promoter region of *IPD3* using the *Agrobacterium rhizogenes* transformation system. The development of nodules on the transformed roots of the mutant plants invaded by *S. meliloti* confirmed that the *IPD3* was impaired in 9F. Since the 9F mutant had a deletion in the *IPD3* gene which caused the mutant phenotype we renamed this mutant *ipd3-1*.

In order to clone the mutated gene in 14S we extended the mapping population up to 650 individuals. The fine mapping experiments resulted in identification of two flanking genetic markers (TC113605F1/R1 and 3g110410F1/R1) that show 1-1 recombination to the mutant phenotype. These genetic markers are located in a single BAC contig (series of Bacterial Artificial Chromosome clones that contain large *Medicago* genomic DNA inserts) and the minimum tiling path between the flanking markers consisted of five BAC clones of which four have been already sequenced in the frame of the *Medicago* Genome Sequencing Project ([www.medicago.org/genome/](http://www.medicago.org/genome/)). We initiated the sequencing of the non-sequenced BAC clone mth4-36h23 in the cooperation with the BAY-GEN Institute (Bay Zoltán Alkalmazott Kutatási Közalapítvány). We have carried out bioinformatic analysis of the gene content of sequenced BAC clones and identified 78 genes or predicted coding sequences. The ineffective mutants have been generated by fast-neutron mutagenesis which causes both small and large deletions. Therefore we have tested primer pairs of 36 genes or predicted coding sequences using PCR 14S and in the allelic mutant *dnf5* but we could not identify a large deletion so far by analyzing the amplified products in agarose gel. We are continuing the testing of other candidate genes and analyzing the amplified fragments with the SSCP technique which is more sensitive to detect small (few base-pair) deletions. When the sequence of the mth4-36h23 BAC clone will be available we will search for deletions in the genes on this BAC.

We have raised the number of F2 plants more than 400 to identify the map position of the 7Y mutant locus more precisely. The mutant locus has been positioned between genetic markers EF414291F1/R1 and h2\_96b16t19F1/R1. These genetic markers are located in two neighboring BAC clones (mth2-62p5 and mth2-96b16) in 154 kb distance. We finished the bioinformatic analysis of these two BAC clones to identify candidate genes for identification and we are analyzing PCR products of 22 genes or predicted coding sequences to identify mutation in them.

Cloning with Affymetrix gene chip: in cooperation with J. Murray and M. Udvardi in the Noble Foundation (Ardmore, Oklahoma) we have attempted the cloning of the mutant genes in the 5L/11S, 6V, 12AA and 13U by hybridizing the genomic DNA of the mutant plants to the *Medicago* Affymetrix oligonucleotide microarray (gene chip). Previously they used this approach successfully to identify mutant loci in the *M. truncatula* genome. We prepared high quality genomic DNA samples from 6-8 plants/ mutant line which identified from the backcrossed population and pooled their DNA. In this way we wanted to reduce the number of deleted genes detected by the gene chip. Following the hybridization of A17 (wild type) and mutant genomic DNA samples to the Affymetrix microarray we analyzed the probesets that showed reduced 50% of wild type signal in the mutant pool. First the map positions of the potential deletion events

were compared with the location of the mutant loci. We could not detect co-segregation of any detected deletion with the 5L mutant gene but the analysis of the hybridization data of the 11S mutant revealed two deletions which co-segregated with the mutant locus. Analyzing the *M. truncatula* genomic sequence we found that the two candidates for the deletion, a glycine rich protein (*GRP*) and a sulfate transporter gene (*SST1*) are located next to each other. PCR analysis confirmed that both genes are deleted in the 11S mutant and the deletion is delimited to a 30 kb genomic region. The sequence analysis of the *GRP* and *SST1* genes in the 5L mutant (the allele of 11S) identified a 9 bp deletion in the 9th exon of the sulfate transporter gene which confirmed that the mutation of the *SST1* caused the mutant phenotype of 5L and 11S mutants. The homolog of *SST1* has been identified recently in *Lotus japonicus* in which the sulfate transporter is essential for the proper function of the symbiotic nodule (Krussel et al. 2005). We cloned and introduced the wild type allele of *SST1* into 5L and 11S mutant plants by *A. rhizogenes* to confirm the identity of the *SST1* gene.

The Affymetrix gene chip hybridization of 12AA genomic DNA detected deletion in 20 probe sets. Unfortunately only one of them corresponded to a known genomic region of *M. truncatula*, the others reside in the unsequenced part of the genome. The probe sets belonged to five genes or gene family; deletions were detected in a pyrrolin-5-carboxylate synthetase (*P5CS*), in a predicted tropinone reductase, in a predicted serine/threonin-protein kinase, in a lectin-like receptor kinase and in a hypothetical protein. In order to detect co-segregation between the candidate deletions and the 12AA mutant locus we started to map the candidate genes. One of the primer pairs designed for the *P5CS* gene identified a deletion in the 12AA mutant and the genetic mapping of this deletion co-segregated with the mutant phenotype. Based on the EST (expressed sequence tag) sequences the pyrrolin-5-carboxylate synthetase gene has two copies in the *Medicago* genome and the sequence of both copies is incomplete. In order to determine sequence of the *MtP5CS* gene co-segregating with the mutant phenotype we identified the BAC clone mth2-51L1 using an allele specific amplified product. We are carrying out inverse PCR experiments and subcloning the BAC clone to determine the sequence of the *P5CS* gene and the neighboring genomic region to delimit the deletion in 12AA. We also plan to test whether the mutation in the *P5CS* gene is caused the mutant phenotype.

We also attempted the identification of the mutant genes in the case of 13 and 6V mutants. The analysis of 13U hybridization data revealed a cDNA sequence of a nodulin gene which is presumably deleted in the mutant plant. The PCR analysis proved that this nodulin is deleted in 13U and the deletion was linked to the mutant phenotype. Unfortunately the gene resides in a non-sequenced region of the *M. truncatula* genome therefore we identified the BAC

clone (mth2-28o5) containing the nodulin gene using a PCR-based method. In order to determine the entire sequence of the nodulin-like gene and delimit the size of the deletion we started the sequencing of the mth2-28o5 BAC clone. The analysis Affymetrix gene chip data of 6V mutant also revealed a deletion which co-segregated with the mutant phenotype. We could detect the boundary of the large, appr. 70 kb deletion in 6V mutant which contains couple of genes and predicted coding sequences as we found following the analysis of the gene content of the mh2-5n3 BAC clone. A bit larger deletion was detected in the *dnf7*, in the allele of 6V, (see Table 1) which proved that the mutated gene in 6V/*dnf7* sought for is located in this genomic region. We have started to clone the genes in the deleted region into binary vectors and we will introduce them into mutants plants with *A. rhizogenes* transformation system to perform genetic complementation and find which gene is responsible for the mutant phenotype.

*The positional and Affymetrix gene chip-based cloning identified the IPD3 and SST1 genes impaired in the 9F (ipd3-1) and 5L/11S (sst1-1 and sst1-2) mutants. Affymetrix gene chip hybridization provided us with deletions co-segregating with the mutant phenotype in the case of 6V, 12AA and 13U mutant plants. Genetic complementation experiments will identify the Fix genes in these mutants in the near future. The positional cloning experiments defined the genomic regions containing the mutated Fix genes in 7Y and 14S mutant plants.*

### **Characterization of the IPD3 gene and the functional analysis of its gene product**

IPD3 was identified earlier as an interactot of CCaMK in yeast two-hybrid systems in *M. truncatula* (Messinese et al. 2007). The Ca<sup>2+</sup>/calmodulin-dependent protein kinase (CCaMK) is a member of the common signaling pathway of nitrogen fixing and arbuscular mycorrhiza (AM) symbiosis and involved in Nod factor (NF) signal transduction. Therefore we further investigated the *ipd3-1* mutant whether it shows similar phenotype as *M. truncatula ccamk* symbiotic mutants and shows similar features in symbiotic responses.

In cooperation with G. Oldroyd (JIC, Norwich, UK) we investigated the AM symbiotic phenotype of *ipd3-1* plants. In contrast to the *ccamk* mutant no defects were found in colonizing fungal structures in *ipd3-1* but the frequency of colonization was significantly reduced in the *ipd3-1* line compared to wild type roots. To assess whether the CCaMK interacting partner IPD3 is required for nodulation gene expression, we analyzed the expression of three Nod factor and rhizobia inducible genes in *ipd3* mutants. In order to analyze the NF induction of *ENOD11* expression a GUS reporter gene driven by the *ENOD11* promoter (Journet et al., 2001) was introduced into the *ipd3-1* mutant background. *ipd3-1* and wild type seedlings containing the

reporter gene construct were continuously treated with NF for 24 h and subsequently monitored for GUS activity. In wild type plants GUS activity was detected in the epidermis of the NF responsive region but GUS activity in *ipd3-1* mutants was restricted to a smaller region than wild type indicating defects in the NF signal pathway in *ipd3-1* mutants. To further analyze the NF induced *ENOD11* expression and test the function of IPD3 during the early stages of the symbiotic interaction we analyzed the induction of *ENOD11*, *HAP2* and *NIN* gene expression following 16 hours of NF treatment by quantitative real-time PCR. We used other mutant alleles of *ipd3-1* (*ipd3-2* and TE7) identified in other studies in the expression studies to validate the expression data. As previous studies demonstrated (Catoira et al. 2000; Oldroyd and Long 2003), *DMI2* and *NSP2* are required for the NF induced *ENOD11* expression thus no or reduced induction of *ENOD11*, *HAP2* and *NIN* was detected in *dmi2* and *nsp2* mutants (Fig. 8A-C). Based on the symbiotic phenotype and the ability of spontaneous nodule formation of *lin* (Kuppusamy et al. 2004 and Kiss et al. 2009), the NF signal transduction pathway is predicted to be unaffected in *lin* and accordingly *ENOD11*, *HAP2* and *NIN* were strongly induced in *lin* similarly as wild type (Fig. 3A-C). As presented in Fig. 3A significant reduction of NF inducible *ENOD11* expression was detected following 16 h NF treatment in the *ipd3-1* mutant and the other *ipd3* mutant plants showed similar expression pattern as *ipd3-1*. Not a strong reduction but a lower relative transcript level of *NIN* and *HAP2* was detected in the three *ipd3* mutants (Fig. 3B and C). To examine the effects of bacterial inoculation on the expression of these marker genes we monitored their relative transcript level in wild type and *Mtipd3* mutant plants after one, eight and fourteen days of inoculation with *S. meliloti*. Following one day of inoculation the *ipd3-1* and TE7 mutants exhibited reduced expression of *ENOD11* and *NIN* (Fig. 3D and E). No induction of *HAP2* was detected (Fig. 3F) in neither of tested plants at one day which is in accordance with the expression pattern of *HAP2* detected previously by Combier et al. (2006). Following eight and fourteen days the induction level of *ENOD11* was similar in mutants and wild type plants (Fig. 3D) while the induction of *NIN* was slightly reduced in *Mtipd3-1* and *Mtsym1* mutants compared to wild type. The expression level of *MtHAP2* was significantly reduced both at 8 and 14 days post inoculation indicating the defects of high number of primordia-like nodules on the roots of *ipd3* mutant plants.

Our results indicate that the expression of *ENOD11*, *NIN* and *HAP2* is impaired in *ipd3* mutants following 16 hours of NF treatment. The expression analysis of early induced nodulin genes showed that *IPD3* is not essential for the expression of *ENOD11* and *NIN* genes involved in the NF signal transduction pathway at later time points but they imply the function of IPD3 in the expression of a *HAP2* necessary for nodule cell differentiation.

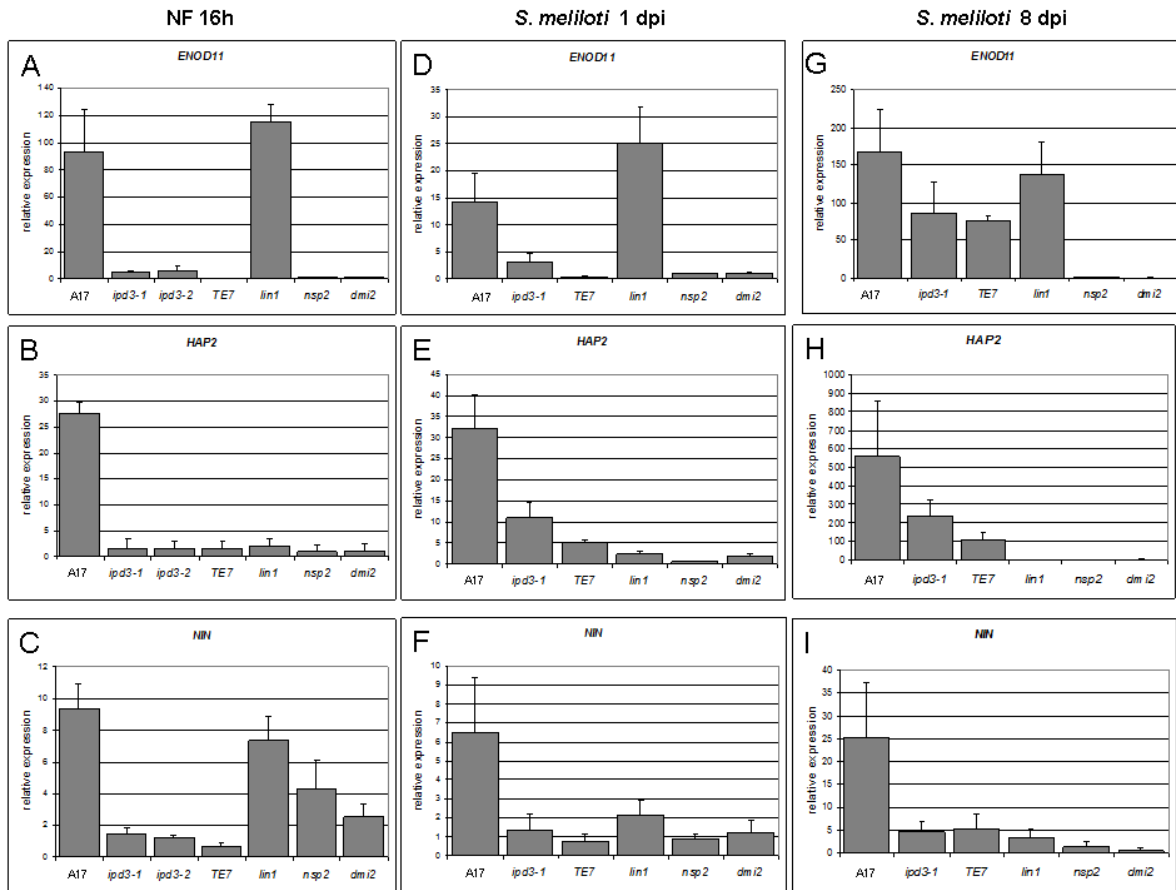


Figure 3. *ipd3* mutants show defects in Nod factor induced gene expression but it is not essential for early nodulin gene expression following 8 and 14 days of inoculation of *S. meliloti*. Relative transcript level of *ENOD11*, *HAP2* and *NIN* genes in wild type (Jemalong) and mutant plants were calculated in relation to non-treated (A-C) wild type plants or 1 day old (D-F) inoculated wild type plants using quantitative real time PCR following 16 hours of Nod factor treatment (A-C), one, eight and fourteen (D-F) days post inoculation with *S. meliloti* 1021. Error bars represent SE.

The further characterization of the *ipd3-1* mutant showed that effectiveness of the AM colonization significantly reduced but no severe defect could be found in the AM symbiotic structures. The nodulation and AM symbiotic phenotypes suggest that *IPD3* functions in the accommodation of the symbiotic partners in the host cells. Expression data also suggest that *IPD3* acts in the NF signal pathway. The function of *IPD3* in NF signal transduction and the symbiotic phenotype of *ipd3* mutants suggest that the components of the common symbiotic signaling pathway is functioning not only during the early steps but during the later stages of the symbiotic interaction too.

## Publication of the results

The preparation of two manuscripts containing (1) the genetic and phenotypic characterization of the *M. truncatula* ineffective mutants and the cloning of the *SST1* gene and (2) the cloning the functional analysis of *IPD3* is in progress. The cloning the other mutants will be continued and the results will be published afterwards.

## References

- Catoira, R, Galera C, de Billy F, Penmetsa RV, Journet EP, Maillet F, Rosenberg C, Cook D, Gough C, Dénarié J (2000) Four genes of *Medicago truncatula* controlling components of a Nod factor transduction pathway. *Plant Cell* 12:1647-1665.
- Combiér JP, Frugier F, de Billy F, Boualem A, El-Yahyaoui F, Moreau S, Vernie T, Ott T, Gamas P, Crespi M, Niebel A (2006) MtHAP2-1 is a key transcriptional regulator of symbiotic nodule development regulated by microRNA169 in *Medicago truncatula*. *Genes & Development* 20: 3084-3088
- Oldroyd GED, Long SR (2003) Identification and characterization of nodulation-signaling pathway 2, a gene of *Medicago truncatula* involved in Nod factor signalling. *Plant Physiology* 131: 1027-1032
- Journet EP, El-Gachtouli N, Vernoud V, de Billy F, Pichon M, Dedieu A, Arnould C, Morandi D, Barker DG, Gianinazzi-Pearson V (2001) *Medicago truncatula* ENOD11: A novel RPRP-encoding early nodulin gene expressed during mycorrhization in arbuscule-containing cells *Mol Plant-Microbe Interact* 14: 737-748
- Krussel, L, Krause, K, Ott, T, Desbrosses, G, Kramer, U, Sato, S, Nakamura, Y, Tabata, S, James, EK, Sandal, N, Stougaard, J, Kawaguchi, M, Miyamoto, A, Suganuma, N, Udvardi, M (2005) The sulfate transporter *SST1* is crucial for symbiotic nitrogen fixation in *Lotus japonicus* root nodules. *Plant Cell* 17:1625-1636.
- Kuppusamy KT, Endre G, Prabhu R, Penmetsa RV, Veereshlingam H, Cook DR, Dickstein R, VandenBosch KA (2004) LIN, a *Medicago truncatula* gene required for nodule differentiation and persistence of rhizobial infections. *Plant Physiology* 136: 3682-3691
- Kiss, E, Oláh, B, Kaló, P, Morales, M, Heckmann, AB, Borbola A., Lózsa, A., Kontár K., Middleton, P, Downie, J.A. Oldroyd, G.E.D. and Endre, G. (2009) LIN, a novel type of U-box/WD40 protein, controls early infection by rhizobia in legumes. *Plant Phys* 151: 1239-1249
- Messinese E, Mun JH, Yeun LH, Jayaraman D, Rouge P, Barre A, Lougnon G, Schornack S, Bono JJ, Cook DR, Ane JM (2007) A novel nuclear protein interacts with the symbiotic DMI3 calcium- and calmodulin-dependent protein kinase of *Medicago truncatula*. *Mol Plant-Microbe Interact* 20: 912-921
- Starker CG, Parra-Colmenares AL, Smith L, Mitra RM, Long SR (2006) Nitrogen fixation mutants of *Medicago truncatula* fail to support plant and bacterial symbiotic gene expression. *Plant Physiology* 140: 671-680